An Analysis of Fatigue Crack Path in Welded Rails

S. Beretta, M. Boniardi, M. Carboni and H. Desimone

Politecnico di Milano, Dipartimento di Meccanica, via La Masa 34, 20158 Milano, Italy
stefano.beretta@polimi.it - marco.boniardi@polimi.it
michele.carboni@mecc.polimi.it - hernan.desimone@polimi.it

ABSTRACT. *Some typical fatigue failures of butt-welded rails consist in fractures of the web. In the early stage, crack propagates parallel to rail surface but, after a while, it tends to propagate with a slant surface. The aim of the present work is to analyse the mechanisms involved in crack propagation in rail's web in order to be able to predict the crack path and, in a second step, the rail inspection intervals. From this point of view, FEM analyses of an observed fracture were carried out in order to determinate* K_I *and* K_{II} *history at different positions of crack tip during the passages of the typical loads induced by trains. The results have shown that the initial flaw tends to follow a path where* ΔK_{II} *is close to maximum values and a small superimposed* K_I *traction is present. Fractographic analyses have confirmed that propagation is mainly controlled by mode II and that mode I is prevalent only after the final bifurcation of the cracks.*

INTRODUCTION AND FAILURE DESCRIPTION

In-service failures of rails are in general related to surface cracks along the treads or, less frequently to cracks at the butt-welds. Figure 1 shows some typical crack failures starting from welded joints [1]. As it can be observed in Fig. 1a and 1b, the crack path is characterised by a first part where the flaw grows almost parallel to the surface and a second part where it presents two kinking angles: at the leading tip (in the rolling direction sense) the crack grows towards the rail tread, at the trailing tip, instead, the crack grows towards the rail base. Figure 1c, in turn, shows the schematisation of a crack that starts its growth parallel to the surface and then it exhibits two branches, both at the leading and trailing tips.

The described change in crack path suggested that, in these failures, firstly cracks grow under mode II and then, at the kinking or branching point, they switch growing to mode I. Several cracks produced by rolling contact fatigue, due to wheel/rail contact, have been reported in literature [2-6]. In these cases, mode II propagation has been assessed and it's proven [7] that this crack propagation mode is enhanced by the high compression stresses due to contact. However, the failures here considered are located at level of the web where the compression stresses are not so important because of the distance from the contact affected zone.

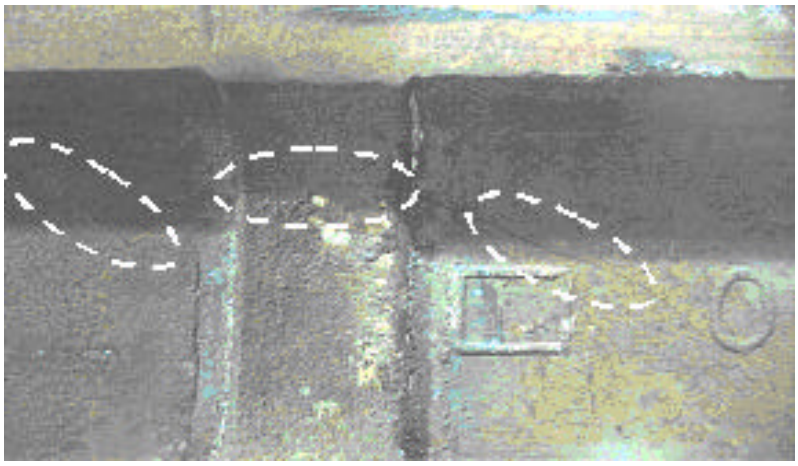

(a)

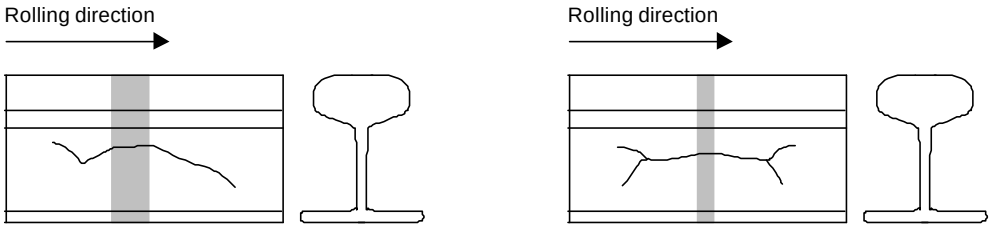

(b) (c)

Figure 1. a) and b) crack with two kinking and its schematisation; c) schematisation of another typical crack presenting branching.

As in the cases of surface cracks started by rolling contact fatigue, a downward crack branching or kinking may lead to fracture of the whole rail and to danger of derailment [8], so it is important to analyse the criteria governing crack branching. Indeed, if a mode II propagation in the first part of the crack is confirmed, it would be important to analyse the criteria used to decide the place of welding joints along the rail.

FRACTOGRAPHIC OBSERVATIONS

In order to understand the fracture mechanism, SEM observations were carried out. In all the considered samples, the fracture surfaces were damaged by frictional rubbing and wear of the opposing surfaces themselves, as reported by Wong [8]. Thus, in practice, it was neither possible to identify the crack nucleation point nor the fatigue striations. For this reason, the surface was cut along its symmetry axis, as it can be seen

in Fig. 2a. Then, after polishing the inner face, the specimens were observed by SEM, in order to see the main properties of the crack path.

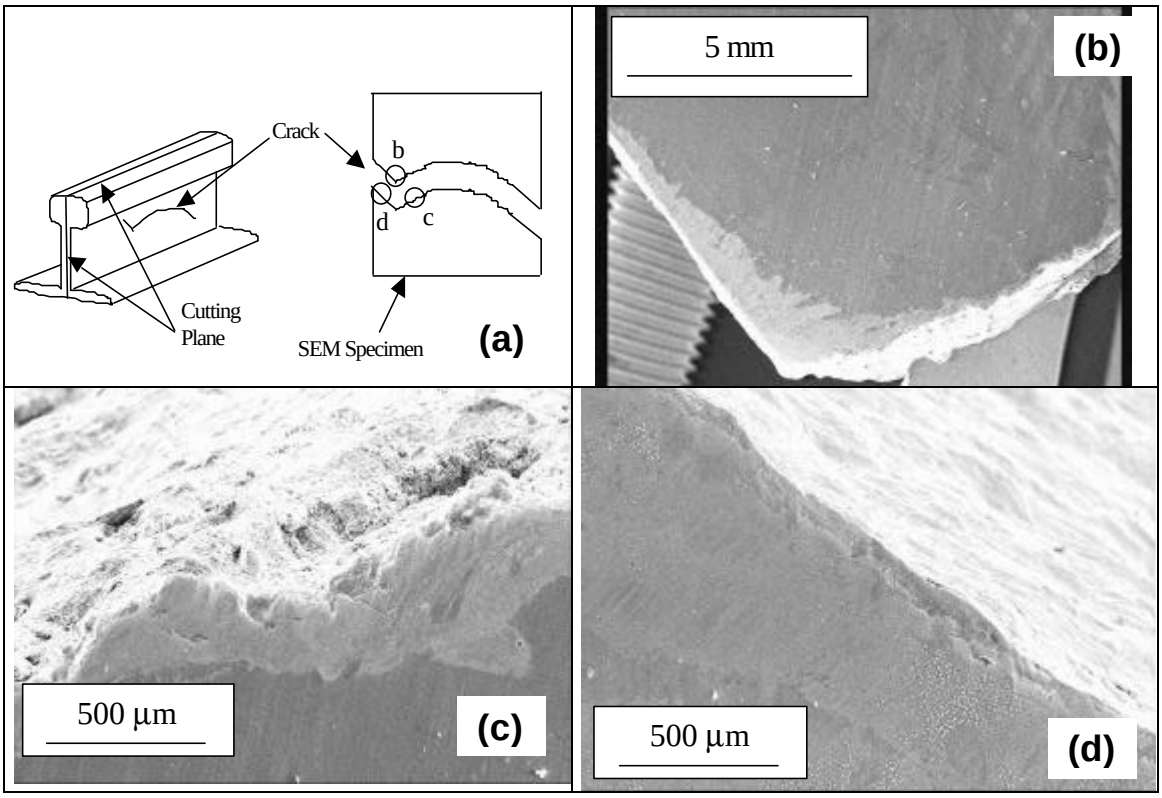

Figure 2. SEM analyses of the leading kinking region: a) general view of cracked rail; b) the kinking; c) surface fracture before the kinking; d) surface fracture after the kinking.

Figures 2b shows the crack path before and after the kinking. It can be noted that before the kinking (Fig. 2c), the fracture surface shows a high damaged pattern while, after the kinking (Fig. 2d), the damage strongly decreases. It has been reported in literature [9,10] that mode II is associated with a higher level of plasticity damage and short branching. This observation seems to support the starting hypothesis: the change in damage pattern can be associated with the change of crack propagation mode, from a starting mode II to a final mode I.

Figure 3 shows the SEM photographs for the central part of the crack (nucleation region). It can be seen, once again, a high level of damage associated with the propagation. Furthermore, Figure 3d shows a secondary fracture surface presenting a stepwise pattern: this is a typical kind of damage associated with mode II propagation [11,12].

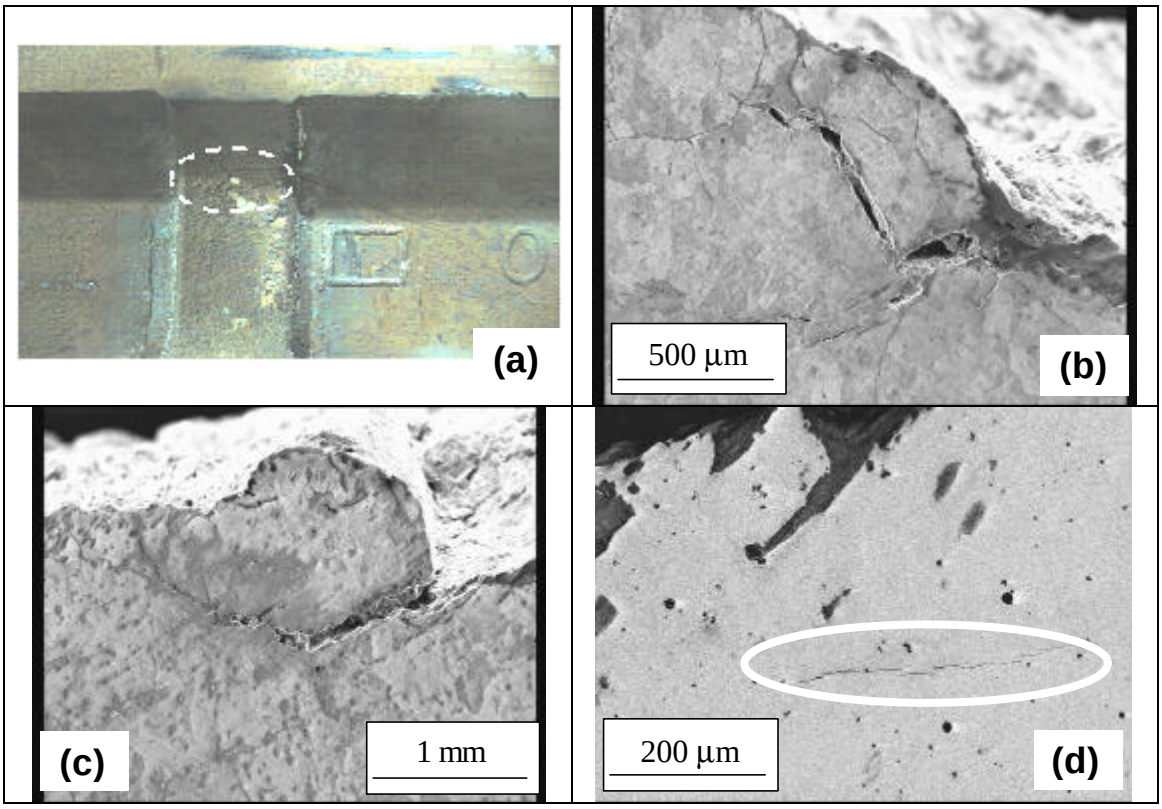

Figure 3. SEM analyses of fracture at the welded joint: a) examined region; b) and c) mode II damage on the fracture surface; d) a secondary crack showing a stepwise pattern.

FEM ANALYSYS

General Description

In order to confirm the hypothesis of a first mode II propagation followed by branching or kinking transition to mode I, 3D FEM analysis were carried out using the commercial finite element package ABAQUS Version 6.2 [13]. 20-node solid elements have been used and crack surfaces contact was introduced by master-slave surface method. Figure 4 shows the finite element mesh for the first step. K_I and K_{II} values at the crack tip were obtained from relative crack opening displacement ΔU_z and sliding displacement ΔU_x of crack nodes, by means of well known formulations [14]:

$$K_I = \frac{2\pi G \Delta U_z}{(3-4\nu)\sqrt{2\pi L}} \qquad as \quad L \to 0 \qquad (1)$$

$$K_{II} = \frac{\pi G \Delta U_x}{2(1-\nu)\sqrt{2\pi L}} \qquad as \quad L \to 0 \qquad (2)$$

where G is the shear modulus, ν is the Poisson's ratio and L is the distance from the crack tip. The variation of K_I and K_{II} for leading crack tip with various positions of the wheel is shown in Fig. 5. The local K_I and K_{II} for a prospective α kinking angle are obtained by [14]:

$$\underline{K}_I(\alpha) = C_{11}K_I + C_{12}K_{II} \tag{3}$$

$$\underline{K}_{II}(\alpha) = C_{21}K_I + C_{22}K_{II} \tag{4}$$

where $\underline{K}_I(\alpha)$ and $\underline{K}_{II}(\alpha)$ are the local stress intensity factors at the tip of the kink and K_I and K_{II} are the stress intensity factors for the main crack, obtained by FEM analysis and Eqs 1 and 2. The coefficients C_{ij} are given by:

$$C_{11} = \frac{3}{4}\cos\left(\frac{\alpha}{2}\right) + \frac{1}{4}\cos\left(\frac{3\alpha}{2}\right) \tag{5a}$$

$$C_{12} = -\frac{3}{4}\left[\sin\left(\frac{\alpha}{2}\right) + \sin\left(\frac{3\alpha}{2}\right)\right] \tag{5b}$$

$$C_{21} = \frac{1}{4}\left[\sin\left(\frac{\alpha}{2}\right) + \sin\left(\frac{3\alpha}{2}\right)\right] \tag{5c}$$

$$C_{22} = \frac{1}{4}\cos\left(\frac{\alpha}{2}\right) + \frac{3}{4}\cos\left(\frac{3\alpha}{2}\right) \tag{5d}$$

For each angle and for each simulated step (in Fig. 5 is only represented the case of α=0, that means no kinking), two main values are obtained: ΔK_{II} and ΔK_I. For the last one, ΔK_I, crack closure phenomena is neglected.

Crack Growth Direction

Several FEM simulations were carried out for different steps of crack propagation. Figure 6 shows, for the rail failure represented on Fig. 1a, the three simulated crack tip positions. Figures 7 to 9 show the results for the leading tip. In all cases, α represents the angle between possible kinking and the present direction of the crack: $\alpha=0$ means non deviation (Fig. 6). At the first and second step, it could be appreciate (Figs 7 and 8) that propagation is associated with a maximum level of ΔK_{II} together with a small K_I. In particular, the actual direction of propagation corresponds to a ΔK_{II} value near to the maximum one which is "helped" by a small K_I. Figure 9, in turn, shows the results for the stress intensity factors when the crack is just before kinking. As it can be observed, the real angle of propagation corresponds to maximum mode I, so it is clear that kinking

is produced in order to change mode II propagation in mode I propagation. Similar results were obtained for the trailer tip.

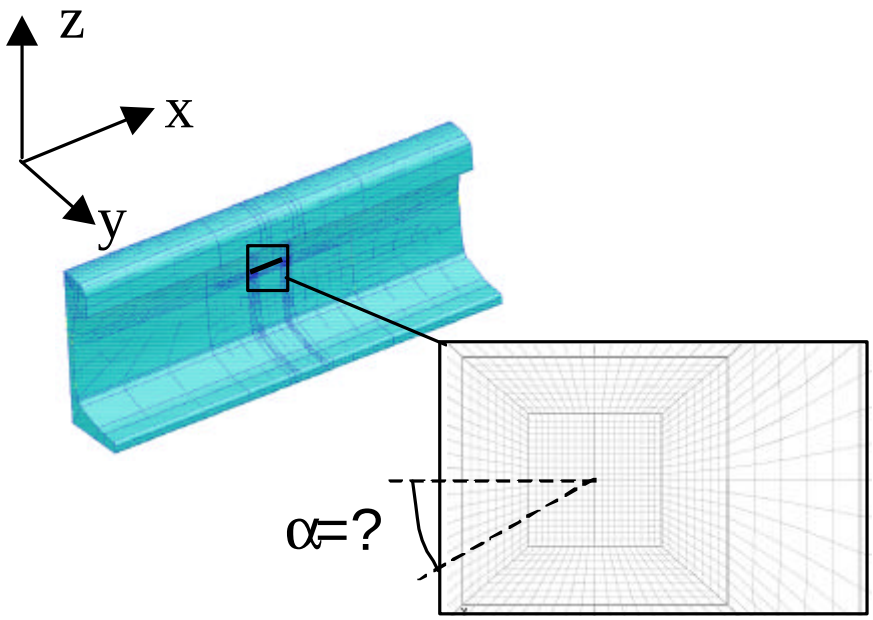

Figure 4. Finite Element Mesh.

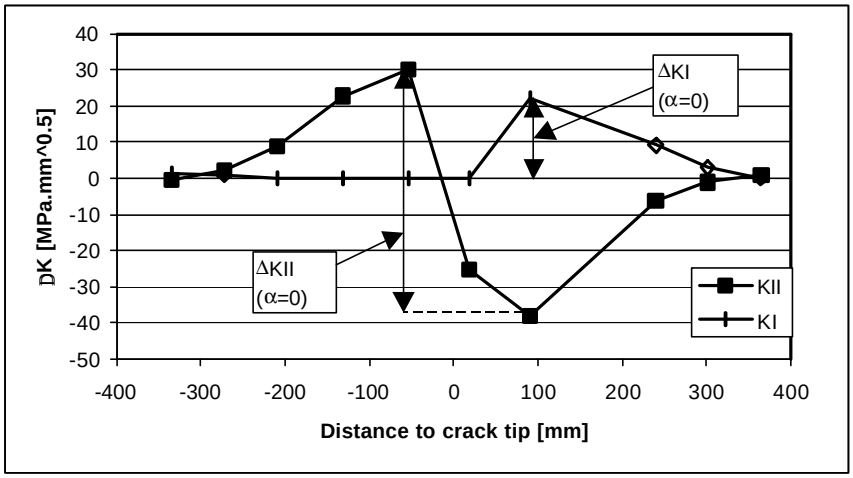

Figure 5. Variation of stress intensity factors with different position of the wheel load.

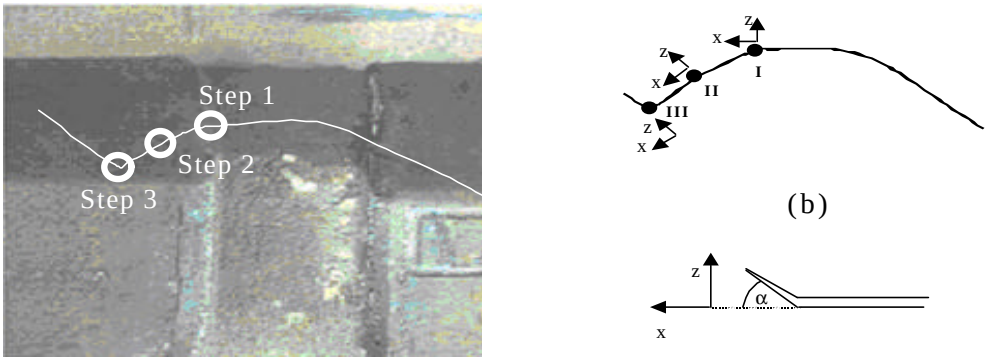

Figure 6. a) Analysed points for the leading tip; b) the convention for co-ordinate axes; c) convention for kinking angle "α".

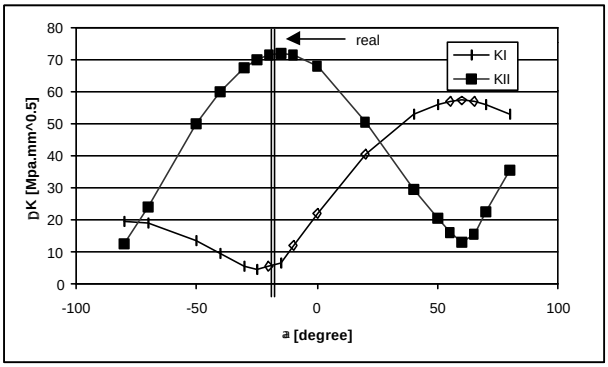

Figure 7. Leading tip at Step 1: Variation of K_I and K_{II} with the kink angle.

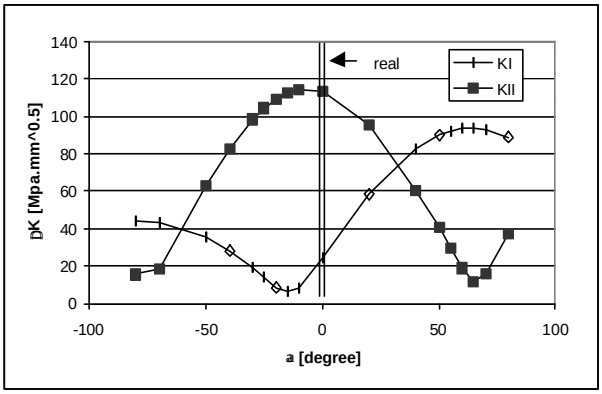

Figure 8. Leading tip at Step 2: Variation of K_I and K_{II} with the kink angle.

CONCLUDING REMARKS AND FUTURE WORK

The propagation of fatigue crack paths in welded rails have been analysed. It was confirmed, by both SEM observations and Finite Element analysis, that this kind of

crack, starting from welded joint, propagates firstly in mode II and then, by a crack path deviation realised in a kinking or branching, switches to mode I propagation.

As the starting mode of propagation is mode II, it would be important to analyse the influence of the position of the welded joint in the rail on the variation of DK_{II}. In all the cases considered here, the weld were always at the middle between two sleepers. Furthermore, it would be important to analyse crack grow rate, in order to define the inspection intervals for welded rails.

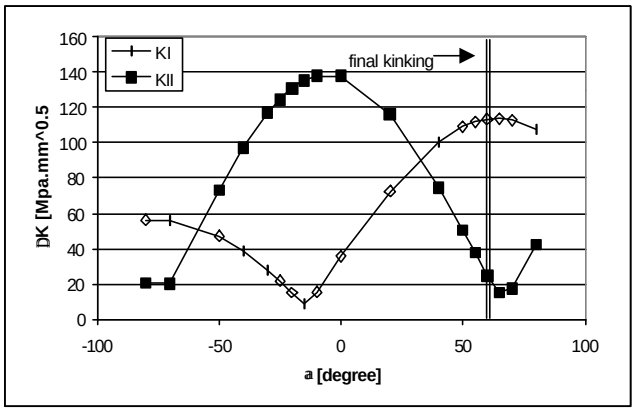

Figure 9. Leading tip at Step 3: Variation of K_I and K_{II} with the kink angle (the final kinking angle maximises K_I).

REFERENCES

1. Kondo, K., Yoroizaka, K. and Sato, Y.(1996) *Wear* **191**, 199-203.
2. Ishida, M. and Abe, N. (1996) *Wear* **191**, 65-71.
3. Akama, M. and Mori, T. (2002) *Wear* **253**, 35-41.
4. Bold, P.E., Brown, M.W. and Allen, R.J. (1991) *Wear* **144**, 307-317.
5. Bogdanski, S. and Brown, M. W. (2002) *Wear* **253**, 17-25.
6. Jung-Kyu, Kim and Chul-Su, Kim (2002) *Materials Science and Engineering* **A338**, 191-201.
7. Melin, S. (1986) *Int. Journal of Fract* **30**, 103-114.
8. Wong, S.L, Bold, P.E., Brown, M.W. and Allen, R.J. (1996) *Wear* **191**, 45-53.
9. Murakami, Y. and Takahashi, K. (1998) *Fatigue Fract. Engng Mater Struct* **17**, 201-219.
10. Murakami, Y, Sakae, C. and Hamada, S. (1999) In: *Fracture*, pp.473-485, Beynon, J.H. (Ed.), Balkema, Rotterdam.
11. ASM Metal Handbook (1997) Ninth Edition, Vol 12, Fractography.
12. ASM Handbook (1996) Vol 19, *Fatigue and Fracture*.
13. ABAQUS (2000) User's Manual. Hibbit, Karlsson & Sorensen Inc.
14. Anderson, T.L (1995) *Fracture Mechanics*, CRC Press, Boca Raton.